# On the Variability of the Mediterranean Outflow Water in the Atlantic Ocean

## Part II: Description of the Mechanism Driving the MOW Variability

Alexandra Bozec[1], M. Susan Lozier[2], Eric P. Chassignet[1]

1: Center for Ocean and Atmospheric Predictions Studies, Florida State University, Tallahassee, Florida
2: Earth and Ocean Sciences, Nicholas School of the Environment, Duke University, Durham, North Carolina

Corresponding Author:
Alexandra Bozec
COAPS Florida State University
227 RM Johnson Building
2035 E Paul Dirac Dr
Tallahassee, FL-32310
USA
Tel: 850-645-1253
Fax: 850-644-4841
abozec@coaps.fsu.edu

**Abstract:**

The variability and pathways of Mediterranean Outflow Water (MOW) in the North Atlantic have been a source of debate for several decades. Part I of this study showed that MOW property variability between 1948 and 2006 in the region west of Cadiz can be imputed to Atlantic Ocean circulation changes that result from variable atmospheric forcing. In part II of this study, we investigate how the interannual North Atlantic atmospheric forcing induces the circulation change. Toward that end, we perform a series of simulations that separate the mechanical effect of the wind from the impact of buoyancy forcing. The results show that MOW property variability can be attributed to shifts between its dominant northward and westward pathways. The pathway shifts from predominantly northward between 1950 and 1975 to predominantly westward between 1975 and 1995 and finally back to northward after 1995. Significantly correlated with the North Atlantic Oscillation, these pathway shifts are caused by the combined impact of wind and buoyancy forcing on the circulation of the North Atlantic. As a consequence of the pathway shifts, MOW variability along the westward pathway is out of phase with the MOW variability along the northern pathway, especially in the Rockall Trough.

KEYWORDS: Mediterranean Outflow Water, Long-term Variability, North Atlantic Ocean, Pathway Shifts, Atmospheric Forcing.

## 1. Introduction

The Mediterranean Outflow Water (hereafter MOW) is formed from the mixture of North Atlantic Central Water (NACW) and Mediterranean Sea Water (MSW) along the northern slopes of Gulf of Cadiz. Reaching a buoyant depth around 1100 m, MOW spreads into the North Atlantic: westward to the central Atlantic and northward following the coasts of Portugal and Spain toward the Bay of Biscay and the Rockall Trough, before possibly reaching the Nordic seas [*Reid*, 1978, 1979, 1994; *Lozier et al.*, 1995; *Iorga and Lozier* 1999a, b]. The signature of MOW salinity can be observed as far west as Bermuda and as far north as the Rockall Trough (Figure 1). The wide spread of this warm and salty water mass makes it an important contributor to the heat and salt content of the North Atlantic [*Zenk,* 1975*; Reid,* 1979]. The MOW has also been cited as a possible contributor to the preconditioning of deep water mass formation in key areas of the global thermohaline circulation such as the Labrador and Nordic seas [*Reid,* 1979*; Lozier et al.,* 1995*; McCartney and Mauritzen,* 2001*; Lozier and Stewart,* 2008]. Investigating the evolution of the MOW properties between 1955 and 1993, *Potter and Lozier* [2004] calculated the MOW temperature and salinity trend in a region west of the Gulf of Cadiz defined as the reservoir [10ºW, 20ºW, 30ºN, 40ºN]. During this time period, they found a positive temperature trend (0.101 ± 0.024 ºC/decade), which far exceeds the average North Atlantic temperature trend [*Levitus et al.*, 2000], and a positive salinity trend of 0.028 ± 0.0067 psu/decade. A more recent study by *Leadbetter et al.* [2007] compared the results of a WOCE transect repeated along 36ºN in 1959, 1981, and 2005 between 10ºW and 20ºW. Their findings are consistent with those of *Potter and Lozier* [2004] (i.e., a warming/salinification in the transect between 1959 and 1981).

However, *Leadbetter et al.* found a cooling/freshening along the transect between 1981 and 2005.

There are three possible sources for the variability of the MOW properties in the reservoir: (1) a change in the MSW properties, (2) a change in the NACW properties, or (3) a change in the circulation of the North Atlantic that would shift the MOW water mass distribution in the reservoir. *Lozier and Sindlinger* [2009] showed that the first two possibilities, namely MSW and NACW variability, are too weak to explain the variability of the MOW. The main goal of this study is to understand the variability of the MOW in the North Atlantic by investigating the third possible source.

In part I of this study [*Bozec et al.,* 2010] (this issue), we tested the viability of the third hypothesis by setting up two 59-year simulations of a 1/3º North Atlantic configuration of the HYbrid Coordinate Ocean Model (HYCOM): one with climatological atmospheric forcing and one with interannual atmospheric forcing from 1948 to 2006. Since the model resolution is too coarse to resolve the physical processes of the overflow in the Gulf of Cadiz, the model was combined with the Marginal Sea Boundary Condition box model [MSBC, *Price and Yang*, 1998]. *Bozec et al.* [2010] found that the simulation with interannual atmospheric forcing is able to reproduce the observed MOW temperature and salinity trends in the reservoir, despite the fact that the MOW trend at the exit of the Gulf of Cadiz is close to zero (N.B. this result is in agreement with the findings of *Lozier and Sindlinger* [2009] who used observed MSW and NACW properties to determine the MOW trend at the exit of Cadiz). Since the MOW properties remain stable in the climatologically forced simulation, *Bozec et al.*

[2010] concluded that the MOW variability over the last 60 years has been induced by a change in the North Atlantic circulation due to the variability of the atmospheric forcing.

In part II of this study, we investigate how interannual North Atlantic atmospheric forcing affects the MOW property variability. Three simulations are performed to separate the mechanical effect of the wind stress from the impact of buoyancy forcing on the property and flow fields of the Atlantic Ocean: (1) a simulation forced with climatological wind stress and buoyancy forcing, (2) a simulation forced with interannual wind stress and climatological buoyancy forcing, and (3) a simulation forced with interannual wind stress and buoyancy forcing. The evolution of MOW properties and the transport budgets of the reservoir for each simulation are compared to identify changes in the circulation and properties in the MOW. The variability of the water masses present in the North Atlantic is also examined to investigate how the different components of the atmospheric forcing affect water mass pathways in the North Atlantic. Taking into account the mechanism(s) involved and its (their) effect(s) on the MOW pathways, the variability and extent of the MOW western and northern pathways are discussed with an emphasis on the MOW variability in the Rockall Trough region, which is a potential access point for MOW to the Nordic seas.

The paper is organized as follows: background on the MOW pathways is given in section 2 and the ocean model and experimental setup are presented in section 3. Results are discussed in sections 4 through 8 with the main conclusions presented in section 9.

## 2. Background on the MOW Pathways

Previous work on the distribution of MOW in the North Atlantic has identified western and northern pathways. The westward branch of the MOW flow is described by *Reid* [1994] as extending beyond 35ºW, bringing the Mediterranean water to the western North Atlantic basin. However, *Iorga and Lozier* [1999a and b], using hydrographic data covering 80 years and a geostrophic diagnostic model, found a westward flow that mainly re-circulates between 10ºW and 20ºW with no clear advective flow beyond 20ºW. This latter result is consistent with the findings of *Mazé et al.* [1997], who argue that the incursion of saline water into the North Atlantic Ocean interior is made only through the propagation of Meddies and not from a direct advection of MOW.

The northern branch of the flow follows the coasts of Portugal and Spain, enters the Bay of Biscay, and continues northward toward the Rockall Trough [*Reid*, 1979, 1994; *Bower et al.*, 2002]. Whether or not the MOW enters the Nordic seas is a question still under investigation. Several studies [*Reid*, 1979, 1994; *Iorga and Lozier*, 1999a, 1999b] that have combined hydrographic data and geostrophic models have conjectured a northward flow of the MOW in the Rockall Trough, with some studies suggesting that this flow eventually reaches the Nordic seas [*Reid*, 1994]. Other studies present results from models [*New et al.*, 2001] or from observations [*McCartney and Mauritzen*, 2001] showing that the MOW, blocked by the subpolar front, does not reach beyond Porcupine Bank. In a more recent study, *Lozier and Stewart* [2008] tried to reconcile these two points of view (i.e., whether or not the MOW is present in the Rockall Trough) by showing that the incursion of MOW in the Rockall Trough is significantly (anti)correlated with (eastward)westward shifts of the North Atlantic Front between 1950 and 2000. Their results are consistent with *Holliday et al.* [2003] and *Holliday* [2008], who observed a large increase of the salinity anomaly in the upper 900 m (expected depth of the MOW at this latitude) of the Rockall Trough and the Nordic seas after 1996. These authors attribute this salinity increase to a sudden westward shift of the North Atlantic front that allows more water from the eastern Atlantic basin (warmer and saltier) and less water from the western Atlantic basin (cooler and fresher) to enter the Rockall Trough and then to propagate to the Nordic seas. In this study, we extend the effort of ascertaining the western and northern pathways of MOW and their variability.

## 3. Model Configuration and Experimental Setup

Analysis in part II relies on the same model configuration used in part I. HYCOM is configured for the North Atlantic. [*Bleck,* 2002; *Chassignet et al.,* 2003; *Halliwell,* 2004]. The 1/3º resolution model domain extends from 90°W to 30°E and from 20°S to 70°N (Figure 1) and does not include the Mediterranean Sea. The bottom topography is derived from DBDB5 [*National Geophysical Data Center,* 1985]. This model has the particularity to combine pressure coordinates at the surface, isopycnic coordinates in the stratified open ocean, and sigma coordinates over shallow coastal regions. Twenty-eight hybrid layers whose $\sigma_2$ target densities range from 23.50 to 37.48 kg/m$^3$ are used for the vertical discretization. Vertical mixing is provided by the KPP model [*Large et al.,* 1994]. The initial conditions in temperature and salinity are given by the General Digital Environmental Model [GDEM3; *Teague et al.,* 1990]. Relaxation to climatology is applied at the northern and southern boundaries in 10° buffer zones.

Since the variability of the MOW at the exit of the Gulf of Cadiz does not contribute to the MOW variability in the Atlantic [*Bozec et al.*, 2010], we prescribe a constant property Mediterranean outflow at 8.3ºW in the Gulf of Cadiz. The salinity, temperature, and transport values of the MOW are chosen to be the average values of the MSBC MOW salinity, temperature, and transport of the climatological experiment CLIM described in part I: $S$ = 36.2 psu, $T$ = 11 ºC, and the total transport $Tr$ = 4 Sv (1Sv=$10^6$ $m^3/s$). The MOW is "injected" into HYCOM in layers 14 and 15, corresponding to the target densities $\sigma_2$=36.38 $kg/m^3$ and $\sigma_2$=36.52 $kg/m^3$, in which MOW is neutrally buoyant.

Climatological atmospheric forcing is derived from the 1979-1993 ECMWF climatology (ERA15). To account for synoptic atmospheric variability, 6-hourly wind stress anomalies corresponding to a neutral El Niño period (September 1984-September 1985, from the Southern Oscillation Index) are added to the monthly wind stresses; wind speed is obtained from the 6-hourly wind stresses. The heat and freshwater fluxes are calculated using bulk formulae during model simulations. The heat flux is derived from surface radiation, air temperature, specific humidity, wind speed, and model sea surface temperature (hereafter SST). The freshwater flux consists of an evaporation minus precipitation flux (E-P) plus a relaxation to observed surface salinity with a 30-day time scale. Evaporation is calculated from bulk formulae using wind speed, specific humidity, and model SST. Precipitation is given by COADS.

The interannual atmospheric forcing covers a period of 59 years from 1948 to 2006 and is derived from the NCEP/NCAR reanalysis. To be consistent with this climatological forcing, we keep the ERA15 mean fields and add the 6-hourly NCEP anomalies to produce the atmospheric forcing.

Three simulations of 59 years are performed starting from year 30 of CLIM described in part I of this study. REF, the control simulation, is forced by the climatological forcing ERA15. The WIND simulation is forced with the NCEP/NCAR interannual wind stress over the period 1948-2006 and the climatological buoyancy forcing from ERA15. The BUOY+WIND simulation is forced with the interannual NCEP/NCAR wind stress and buoyancy forcing.

## 4. Comparison of Observed and Modeled MOW Variability

To ensure that we reproduce the observed MOW variability in this North Atlantic configuration of HYCOM, we calculate the observed and modeled salinity, temperature, and density trends over the spatial domain defined by 8.3ºW to 25ºW and 32ºN to 42ºN, considered to be the reservoir for MOW (See box 1 in Figure 1). This spatial domain is slightly altered from that used by *Potter and Lozier* [2004] in order to accommodate the slightly larger spread of MOW in the model. The larger MOW spreading area in the model can be attributed to the 4 Sv outflow transport prescribed as the total MOW transport, which is in the upper part of the observed range [3-4 Sv according to *Baringer and Price*, 1997].

Following the same method used by *Potter and Lozier* [2004], we calculate the observed trends in box 1 for the salinity, temperature, and density at 1100 m from 6950 profiles extracted from the hydrographic database HYDROBASE 2 [*Curry*, 2001] for the periods 1955-1993 and 1955-2003 (N.B. The number of observations available over the region between 2003 and 2006 was not sufficient to estimate the trend between 1955 and 2006). The trends for the observed properties and for the property fields from each of the three simulations discussed above are summarized in Tables 1 and 2. The observational trends in box 1 are comparable to the trends found by *Potter and Lozier* [2004] for the period 1955-1993, with a salinity trend of 0.0298±0.0028 psu/decade (coefficient of determination $r^2$=0.76) and a temperature trend of 0.129±0.013 ºC/decade ($r^2$=0.73). Considering the period 1955-2003, we find significantly lower salinity and temperature trends of 0.0190±0.0026 psu/decade ($r^2$=0.53) and 0.097±0.011 ºC/decade ($r^2$=0.64), respectively. This result is consistent with the reversal of the trends found between the period 1959-1981 and the period 1981-2005 by *Leadbetter et al.* [2007].

The modeled trends are derived from the salinity, temperature, and density fields at 1100 m in box 1 over the 59 years of the model's integration (Figure 2). REF presents a slight increase of salinity and temperature over the time period of the simulation. The drift of the model in the region is estimated at 0.0094±0.0012 psu/decade for the salinity and 0.041±0.006 ºC/decade for the temperature. Over the time period from 1955-1993, WIND has a salinity (temperature) trend of 0.0204±0.0014 psu/decade (0.089±0.008 ºC/decade), weaker than the observed trend for this period, but larger than the drift of the model estimated in REF. In the 1955-2003 period, the WIND salinity (temperature) trend remains close to its 1955-1993 trend with 0.0174±0.0011 psu/decade (0.079±0.006 ºC/decade). In BUOY+WIND, however, the observed salinity (temperature) trend is remarkably reproduced for both periods, 1955-1993 and 1955-2003. The salinity (temperature) trend is 0.0312±0.0030 psu/decade (0.143±0.014 ºC/decade) for the 1955-1993 period with a coefficient of determination $r^2$=0.74 ($r^2$=0.73) and 0.0195±0.0026 psu/decade (0.092±0.014 ºC/decade) for the 1955-2003 period with a coefficient of determination $r^2$=0.55 ($r^2$=0.56). From this analysis, it appears that both an interannually varying wind stress and an interannually varying buoyancy forcing are necessary to reproduce the MOW trend in the reservoir.

## 5. Evolution of the MOW Salinity Pattern

To understand why the observed trends are reproduced in BUOY+WIND and not in WIND and REF, the MOW salinity pattern during the period when BUOY+WIND exhibits relatively low salinity (1955-1970) is compared to the salinity pattern during the period when BUOY+WIND exhibits relatively high salinity (1980-1995) (Figure 3). For both of these time periods the salinity is averaged on layers 14 and 15 ($\sigma_2$=36.38 kg/m$^3$ and $\sigma_2$=36.52 kg/m$^3$), the layers in which MOW is introduced into HYCOM.

The comparison of REF salinity patterns between the two periods (Figures 3a, d) shows a freshening west of 30ºW and a salinification south of 30ºN (Figure 3g), illustrating the drift of the model between these two periods. As seen in Figures 3b, e and h, the evolution of the WIND salinity pattern is similar to the evolution in REF, with the exception of a more accentuated salinification in the region from 20-30ºW and 40-50ºN. In BUOY+WIND, there are notable differences from REF and WIND. While the salinification south of 30ºN in the control simulation is also present in this model configuration (Figure 3i), albeit stronger, the freshening west of 30ºW is not. On the contrary, we find a widespread salinification in the central and western portions of the basin. This salinification is readily apparent in the extension of the MOW tongue from the earlier to the later time period: the western extent of the MOW tongue (as measured by the 35.9 psu salinity isoline) is located near 20ºW during 1955-1970 period, yet at 27ºW during 1980-1995 (Figures 3c, f). Such an extension is not apparent in the REF and WIND fields. The salinification in the BUOY+WIND fields finds an exception only near the extended regions of the Gulf of Cadiz and the Bay of Biscay, where freshening is noted, especially for the latter region. Given these strong features, we conjecture that the salinification in the west and freshening in the north (in the Bay of Biscay) are due to a westward expansion of the tongue and consequently its retraction from the north. This possibility is pursued in the following sections.

## 6. Evolution of the Transport in Box 1

To ascertain whether an MOW pathway shift occurred between 1955-1970 and 1980-1995, we analyze the evolution of the transports at each boundary of box 1 (Figure 4). The transport is positive for water flowing out of the box and is calculated for layers 14 and 15. In all cases, the strong transport into the box from the eastern boundary is noted. The relatively stable transport of MOW (~4Sv) into the box is characteristic of all three model runs. The balance to this input is achieved by a combination of output from the northern, southern and western boundaries. Importantly, these outputs vary with each model run, as described below.

The outgoing transports in the climatological simulation REF are relatively stable throughout the simulation. The northward transport is dominant (with an average of 2.17 Sv); the southward and westward transports are close to zero except for the periods 1950-1955 and 1985-2005, when the westward transport is ~1 Sv. In WIND, the transports exhibit larger variations than in REF. The northern transport is also the dominant transport for most of the simulation, with an average of 1.93 Sv compared with an average of 1.20 Sv for the westward transport. Occasionally, the westward transport has a stronger intensity than the northward transport (i.e., during 1950-1955 and 1990-1995). Furthermore, WIND presents a significant anti-correlation between its western and northern transports ($r^2$= 0.80, p<0.01 at lag 0). In BUOY+WIND, the averages of the northward and westward transports are roughly equivalent over the period of the simulation, at 1.51 Sv and 1.65 Sv, respectively. The northern transport is dominant during the 1955-1965 period and after 1995; and the westward transport is generally dominant during 1970-1995. Furthermore, as with WIND, the transports at the northern and western boundaries are strongly anti-correlated ($r^2$=0.79; p<0.01 at lag 0). These results indicate that MOW has preferred pathways (northward or westward) that are temporally variable as seen in WIND and BUOY+WIND and that the dominant MOW pathway has varied between 1948 and 2006.

To see how the variability of the transport relates to the variability of the atmospheric forcing, we calculate the correlation of the transport with the dominant mode of North Atlantic atmospheric variability: the winter North Atlantic Oscillation index (NAO) [*Hurrell*, 1995]. In WIND, none of the transports is significantly correlated to the NAO index. In BUOY+WIND, the NAO index is significantly correlated with the westward transport at lag 0 ($r^2$=0.65; p<0.01) and significantly anti-correlated with the northward transport at lag 0 ($r^2$=0.45; p<0.01). Thus, MOW has a tendency to spread northward during low NAO and westward during high NAO, explaining the salinification in the west and the freshening in the north in the 1980-1995 period compared with the 1955-1970 period. Furthermore, the variability of the westward/northward transport in BUOY+WIND is correlated/anticorrelated with the salinity variability in box 1 ($r^2$=0.72/-0.45; p<0.01), indicating that these shifts in the dominant pathway are responsible for the salinity trend in box 1 observed between 1955 and 2003. Although the mechanical impact of the time varying wind-stress induces an anti-correlation between the northward and westward transport (the northward transport remaining the dominant pathway), time-varying buoyancy forcing is also needed to reproduce the observed MOW variability.

## 7. Impacts of the Pathway Shifts

We next investigate the impact of these pathway shifts on the distribution of MOW in the North Atlantic. We include changes in the thickness and spread of Labrador Sea Water (LSW) in this investigation since LSW and MOW constitute the two major mid-depth water masses in the North Atlantic and the salinity field at mid-depth is intricately linked to the distribution of both of these water masses. Also in the section, the consequences for MOW variability in the Rockall Trough are analyzed.

### 7.1. Variability of MOW Along the Western Pathway

A comparison of the water mass distribution of WIND and BUOY+WIND in the central Atlantic is conducted in the region where the MOW tongue expands to the west of box 1 [30ºW, 40ºW, 30ºN, 40ºN] (box 2, Figure 1). The thickness evolution of each density class between 500 m and 2600 m (here corresponding to ten density classes from $\sigma_2$=36.04 kg/m$^3$ to $\sigma_2$=36.97 kg/m$^3$) is calculated (Figure 5).

WIND shows a weak variability in layer thickness in every density class, except for the LSW densities ($\sigma_2$=36.83 kg/m$^3$ and $\sigma_2$=36.89 kg/m$^3$), which exhibit an increase in the 1960s and again in the 1980s (Figure 5a). The salinity in the MOW density classes ($\sigma_2$=36.38 kg/m$^3$ and $\sigma_2$=36.52 kg/m$^3$) in this region stays quite stable throughout the simulation (Figure 5a, top). In BUOY+WIND, more variability of the MOW density class thickness ($\sigma_2$=36.52 kg/m$^3$) and the LSW density class thickness ($\sigma_2$=36.83 kg/m$^3$) (Figure 5b) than in WIND is apparent. The MOW density class thickness is quite stable between 1950 and 1970; it then increases until stabilizing again in the mid-1980s. After 1995, the MOW density class thickness slightly decreases. In addition, the significant increase in salinity (+0.1psu) after 1970 in the MOW density classes (Figure 5b, top) shows that MOW is responsible for the increasing density class thickness (Figure 5b top). We also note that the increase of the MOW density class thickness in the 1980s coincides with a decrease of the LSW density class thickness over the same period. Since the thicknesses of the density classes located between LSW and MOW density class are staying constant throughout the simulation, we suggest that the variability of the LSW and MOW density class thicknesses are connected. This connection is examined in the following section.

### 7.2. LSW Variability and MOW Pathway Shifts

To understand the variability of LSW and how it relate to MOW pathway shifts, the evolution of LSW density class thickness over the entire North Atlantic is analyzed concurrently with the evolution of the MOW salinity tongue.

In BUOY+WIND, the LSW density class thickness varies strongly during the nearly 60 years of simulation (Figure 6). At the beginning of the simulation (1950-1954), the LSW covers most of the western basin of North Atlantic (north of 40ºN) and part of the eastern basin except for the region east of 25ºW at the latitude of the Bay of Biscay region (40ºN-48ºN). The average thickness of the LSW density class is ~800 m from

65ºN to 45ºN and decreases to an average thickness of less than 300 m south of 40ºN. At the outset, the MOW tongue is strongly constrained to the eastern part of the basin (white contours). Between 1955 and 1969, NAO is in a negative phase and no LSW is formed. Therefore, the thickness of the LSW density class constantly decreases during this period in agreement with the observations [*Curry et al.*, 1998]. The expansion of the LSW however stays similar to the 1950-1954 period. Between 1955 and 1969, the MOW stay constrained at the coast but we notice a northward extension of the salinity contours in the northern part of the Bay of Biscay, in agreement with a preferred northward pathway during low NAO period (See section 6.2).

During the intermediate NAO years (1970-1979), the LSW density class thickness continues to decrease till it reaches an average of less than 400 m over the northern Atlantic. The LSW then starts to retreat from the eastern North Atlantic basin (1975-1979). During that same time period, the MOW salinity contours retract from the northern Bay of Biscay and starts to expand westward to the central Atlantic.

The formation of LSW resumes in the high NAO period (1980-1999) in the Labrador Sea. Starting with moderate water mass formation during 1980-1984, LSW formation is enhanced during 1985-1999 when the thickness of the water mass reaches more than 1000 m over most of the subpolar gyre region, as observed by *Curry et al.,* [1998]. Retreated to the western north Atlantic basin (1985-1989), the LSW progressively refills the North Atlantic and reaches the central Atlantic and the eastern basin in the 1995-1999 period. During the high NAO period, the MOW salinity continues to expand westward to the central North Atlantic region and the salinity contours north of the tongue stays confined to the southern part of Bay of Biscay, which is consistent with a preferred westward pathway during a high NAO period.

After 1995, the NAO is in an intermediate phase; the LSW covers most of the northern Atlantic and has an average thickness of ~800 m as it did at the beginning of the simulation. The MOW is still extended westward during this period; however, we notice a slight retreat of the inner salinity contours toward the east, especially after 2000. At the same time, the salinity contours in the Bay of Biscay shows a northward extension as in the low NAO state. This last result shows that the MOW has as in the 1950-1970 period a preferred northward pathway after 2000.

In WIND, the variability of the LSW density class thickness and spreading area is weaker than in BUOY+WIND over the North Atlantic (not shown). The LSW density class thickness average over the North Atlantic basin presents variations from ~600m (1950-1969 and 1990-2006) to ~900m (1970-1989) and the spreading area stays similar to the BUOY+WIND 1950-1954 spreading area (Figure 6), except for the last 15 years of simulation when a slight northward displacement of the southeastern boundary (near the box 1 region) occurs. During the simulation, the MOW salinity tongue stays confined to the eastern basin with salinity contours extended northward and occasionally westward, in agreement with the variability of the WIND northward and westward transports.

In sum, though the northern and westward pathway shifts are evident in both WIND and BUOY+WIND, only BUOY+WIND reproduces a realistic salinity change in the eastern subtropical basin. We conclude that variable buoyancy forcing is necessary to produce the observed properties of the water masses that are affected by these pathways shifts. Finally, we note that these shifts in the dominant pathway help explain the inconsistencies found in the literature regarding the extent of the western pathway [*Reid*, 1994; *Mazé et al.*, 1997; *Iorga and Lozier*, 1999a and b]. Do these pathway shifts also explain MOW variability along the northern pathway, in particular in the Rockall Trough? This question is next addressed.

### 7.3. Variability of the MOW Along the Northern Pathway

The variability of the MOW salinity along the northern pathway is analyzed by calculating the salinity anomaly averaged over the Rockall Trough [11.5ºW, 15ºW, 52.5ºN, 57.5ºN] (box 3, Figure 1). To highlight the impact of low and high NAO phases on the MOW circulation, we calculate the salinity anomaly relative to the mean salinity between 1955 and 1995.

In the Rockall Trough, BUOY+WIND salinity anomalies vary from an average of ~+0.05 psu in the low NAO phase (1950-1970) to an average of -0.05 psu in the high NAO phase (1975-1995) (Figure 7c). During the two periods of consistently low and high NAO (shaded gray in Figure 7), a higher (lower) northward transport is linked to higher (lower) salinities in the Rockall Trough. Indeed, the correlation between the Rockall Trough salinity and the northern transport of box 1 (Figure 7a) during 1948-1995 is positive (+0.57) and significant ($p<0.01$). The correlation between the Rockall Trough salinity and salinity in box 1 (Figure 7b), where the MOW reservoir resides, is negative (-0.56) and significant ($p<0.01$), in agreement with the pathway shift hypothesis.

After 1995, the salinity in Rockall Trough exhibits a sharp increase (+ 0.2 psu, in agreement with *Holliday* [2003] and *Holliday et al.* [2008]), followed by a decrease after 1999. The transport in box 1 over this time period (from 1995 until 2005) is generally high, in contradiction with the pathway shift hypothesis. Specifically, the salinity decrease after 1999 is not accompanied by a decrease of the northward transports. However, the salinity in box 1, with a gradual decrease after 1995, is in agreement with the northward transports over this time period, and would therefore add credence to the pathway shift hypothesis. Importantly, the gradual decrease in salinity in box 1 is in agreement with observations [*Leadbetter et al.*, 2007]. However, the salinities in box 1 and in the Rockall Trough are no longer significantly anti-correlated if the time frame considered includes the 1995-2006 period.

We suggest that the lack of correlation between the salinity in box 1 and in the Rockall Trough after 1995 might be explained by the fact that NAO is in a "weak" intermediate phase during this period (see Figure 4d), in contrast to the 1950-1970 period (strong negative phase) and the 1975-1995 period (strong positive phase). As such, dynamics other than those associated with NAO may be dominant during this time period.

## 8. Discussion

We have shown that MOW variability in the Atlantic Ocean during the last 60 years depends on the varying northward and westward transports in the eastern North Atlantic and on variable water mass formation. To evaluate how well our model reproduces the water mass transport in the North Atlantic, in particular at depth, we show, in Figure 8, the baroclinic mass transport index (0-2000db) deduced from the anomaly of Potential Energy Anomaly (PEA) between the Labrador Sea and the Bermuda Islands that *Curry and McCartney* [2001] calculated from observations. This transport index represents the eastward transport between the subpolar gyre and the subtropical gyre. We compare the BUOY+WIND transport index with the NAO index and the BUOY+WIND SSH anomaly averaged over the subpolar gyre [60-15ºW, 50-65ºN] (Figure 8c). We find a significant correlation between the BUOY+WIND transport index and the NAO maximum with a 2-year lag ($r^2$=0.71; p<0.01) in agreement with the observations [*Curry and McCartney*, 2001]. We also find a lower but still significant correlation ($r^2$=0.33; p<0.01) with a 2-year lag for WIND (Figure 8b). The transport index averaged over 1950-2000 found by *Curry and McCartney* [2001] is 60 MT/s, and is calculated at 65.9 MT/s in the GDEM3 climatology. The same calculation gives 66.8 MT/s in BUOY+WIND, 74.5 MT/s in WIND and 74.3 MT/s in REF. Though WIND shows a correct variability, the strength of the transport is too high. This is related to the constant buoyancy forcing applied throughout the simulation. This buoyancy forcing is extracted from ERA15, which is a climatology built on the high NAO period 1979-1993. The LSW formation is thus constantly important, enhancing the circulation between the two gyres. These results show that the circulation between the two gyres of the North Atlantic is correctly represented in BUOY+WIND.

## 9. Conclusions

The hypotheses put forward as possible sources of the MOW variability include a change in the Mediterranean Sea Water, a change in the North Atlantic Central Water, or a change of the Atlantic Ocean circulation resulting in a shift of the MOW pathway. *Lozier and Sindlinger* [2009] showed from observations that the variability of MSW and NACW is too weak to explain the observed MOW variability. In part I of this study

[*Bozec et al.*, 2010], we investigated the third possible source of MOW variability in the Atlantic Ocean using an ocean model. We concluded that the MOW variability in the study area defined by *Potter and Lozier* [2004] as the reservoir was driven by a change in circulation of the North Atlantic due to the atmospheric forcing variability between 1948 and 2006.

In part II of this study, we analyze further this change in circulation of the MOW and investigate how the different components of the interannual North Atlantic atmospheric forcing induce the circulation change. Three simulations of 59 years (1948-2006) are performed using a 1/3º North Atlantic configuration of HYCOM: one forced with climatological wind stress and buoyancy forcing, one forced with interannual wind stress and climatological buoyancy forcing, and one forced with interannual wind stress and buoyancy forcing. Only the simulation using interannual buoyancy and wind stress forcing is able to reproduce the observed trends in temperature and salinity of the MOW in the reservoir. The comparison of the mid-depth salinity between 1955 and 1970 and 1980 and 1995 shows a negative salinity anomaly north of the reservoir and a positive anomaly west of the reservoir. The evolution of the MOW transports out of the reservoir helps us conclude that the cause of this extension of the tongue is a shift of the MOW dominant pathway from northward during the 1955-1970 period to westward during the 1980-1995 period. While WIND presents a significant anti-correlation between the northward and westward transport as in BUOY+WIND, the analysis of the evolution of MOW and of the other dominant intermediate water mass of the North Atlantic, LSW, shows that a correct water mass formation and mass transports between the subpolar and subtropical gyre is necessary to induce shifts in the MOW dominant pathway.

As a consequence to the pathway shifts, the evolution of the salinity along the northern pathway, specifically in the Rockall Trough, shows anomalies out of phase with the salinity anomalies found along the westward pathway with positive anomalies between 1950 and 1970 and negative anomalies between 1975 and 1995. After 1995, the MOW salinity in the Rockall Trough increases suddenly by 0.2 psu till 1999 and then decreases till the end of the simulation. While the salinities in the Rockall Trough and in box 1 are strongly anti-correlated for the 1950-1995 period, the (anti-)correlation becomes insignificant when the 1995-2006 period is included in the time frame of the correlation. A possible reason to this result can be the fact that the NAO enters an intermediate "weak" phase after 1995. The atmospheric forcing associated with this phase are therefore weaker than during the two previous strong phases (negative in1950-1970 and positive in 1975-1995), limiting the impact on the MOW variability.

Finally, as our model configuration does not extend further than 70ºN, and as a buffer zone is applied at these boundaries, we cannot draw any conclusions as to whether or not the MOW penetrates the Nordic seas. The average MOW depth in HYCOM is between 600 m and 1000 m in the Rockall Trough, which is mainly below the sill depth of the pathway to the Nordic seas, the Wyville-Thomson Ridge (500-600m). It is therefore unlikely that the Mediterranean Water is able to reach the Nordic seas via this path.

*Acknowledgments.*

This research was supported by the National Science Foundation through grant OCE-0630229. Simulations were performed at the National Center of Atmospheric Research (NCAR), Boulder, Colorado.

## References

Baringer, M. O., & J. Price (1997), Mixing and spreading of the Mediterranean outflow, *J. Phys. Oceanogr*, *27*, 1654-1677.

Bleck, R. (2002), An oceanic general circulation model framed in hybrid isopycnic-Cartesian coordinates, *Ocean Modell*, *37*, 55-88.

Bower, A. S., Lecann, B., Rossby, T., Zenk, W., Gould, J., Speer, K., Richardson, P.L., Prater, M.D., Zhang, H.-M. (2002), Directly measured mid-depth circulation in the northeastern North Atlantic Ocean, *Nature*, *419*, 603-607.

Bozec, A., Chassignet, E.P., Lozier, M.S., And G. R. Halliwell (2010), On the Variability of the Mediterranean Outflow Water in the Atlantic Ocean: Analysis of the source waters variability, *J. Geophys. Oceanogr*., *submitted*.

Chassignet, E. P., Smith, L.T., Halliwell, G.T., Bleck, R. (2003), North Atlantic Simulations with the Hybrid Coordinate Ocean Model (HYCOM): Impact of the Vertical Coordinate Choice, Reference Pressure, and Thermobaricity, *J. Phys. Oceanogr*, *33*, 2504-2526.

Curry, R. G., McCartney, M.S., and T.M. Joyce. (1998), Oceanic transport of subpolar climate signals to mid-depth subtropical waters. *Nature*, *391*, 575-577.

Curry, R., and M.S. McCartney (2001), Ocean Gyre Circulation Changes Associated with the North Atlantic Oscillation, *J. Phys. Oceanogr*, *31*, 3374-3400.

Curry, R. (2001), HydroBase 2: a Database of Hydrographic Profiles and Tools for Cllimatological Analysis, *Technical Reference, Woods Hole Oceanographic Institute,* 81pp.

Halliwell, G. R. (2004), Evaluation of vertical coordinate and vertical mixing algorithms in the HYbrid-Coordinate Ocean Model (HYCOM), *Ocean Modell*, *7*, 285-322.

Holliday, N. P. (2003), Air-Sea interaction and circulation changes in the northeast Atlantic, *J. Geophys. Res*, *108*(C8), doi:10.1029/2002JC001344.

Holliday, N. P., Hughes, S.L., Bacon, S., Beszczynska-Möller, A., Hansen, B., Lavin, A., Loeng, H., Mork, K.A., Østerhus, S., Sherwin, T., and Walczowski, W. (2008), Reversal of the 1960s to 1990s freshening trend in the northeast North Atlantic and Nordic Seas, *Geophys. Res. Let*, *35*(L03614), doi:10.1029/2007GL032675.

Hurrell, J. W. (1995), Decadal Trends in the North Atlantic Oscillation: Regional temperatures and precipitation, *Science*, *269*, 676-679.

Iorga, M. C., And M.S. Lozier (1999a), Signatures of the Mediterranean outflowfrom a North Atlantic climatology 1. Salinity and density fields, *J. Geophys. Res*, *104*(C11), 25985-26009.

Iorga, M. C., And M.S. Lozier (1999b), Signatures of the Mediterranean outflow from a North Atlantic climatology 2. Diagnostic velocity fields, *J. Geophys. Res*, *104*(C11), 26011-26029.

Large, W. G., Mcwilliams, J.C., Doney, S.C. (1994), Oceanic vertical mixing: a review and a model with a nonlocal boundary layer parameterization, *Rev. Geophys*, *32*, 363-403.

Leadbetter, S. J., Williams, R.J., Mcdonagh, E.L., King, B.A. (2007), A twenty year reversal in water mass trends in the subtropical North Atlantic, *Geophys. Res. Let*, *34*(L12608).

Levitus, S., Antonov, J.I., Boyer, T.P., Stephens, C. (2000), Warming of the world ocean, *Science*, *287*, 2225-2229.

Lozier, M. S., And L. Sindlinger (2009), On the source of Mediterranean Overflow Water property changes, *J. Phys. Oceanogr*, *accepted*.

Lozier, M. S., and N.M. Stewart (2008), On the temporally-varying penetration of mediterranean overflow waters and eastward penetration of Labrador Sea water, *J. Phys. Oceanogr*, *38*, 2097-2103.

Lozier, M. S., Owens, W.B., Curry, R.G. (1995), The climatology of the North Atlantic, *Prog. Oceanogr*, *36*, 1-44.

Mazé, J. P., Arhan, M., And H. Mercier (1997), Volume budget of the eastern boundary layer off the Iberian Peninsula, *Deep Sea Res., Part I*, *44*(9-10), 1543-1574.

McCartney, M., And C. Mauritzen (2001), On the origin of the warm inflow to the Nordic Seas, *Prog. Oceanogr*, *51*, 125-214.

National Geophysical Data Center, 1985. Worldwide gridded bathymetry DBDB5 5-min latitude/longitude grid. Data Announcement 85-MGG-01, NOAA/NGDC, Boulder, CO, 75 pp. [Available from NOAA, NGDC, 325 Broadway, E/GC3, Boulder, CO 80303.]

New, A. L., Barnard, S., Herrmann, P., And J.-M. Molines (2001), On the origin and pathway of saline inflow to the Nordic Seas: insights from the models, *Prog. Oceanogr*, *48*, 255-287.

Potter, R.A., and M.S. Lozier (2004), On the warming and salinification of the

Mediterranean outflow waters in the North Atlantic, *Geophys. Res. Lett*, *31*, L01202.

Price, J. F., and J. Yang (1998). Marginal sea overflows for climate simulations. In E. C. a. J. Verron (Ed.), *Ocean Modeling and Parameterization*. (pp. 155-170). Kluwer Academic Publishers.

Reid, J.L. (1978), On the middepth Circulation and Salinity Field in the North Atlantic Ocean, *J. Geophys. Res.*, 83(C10), 5063-5067, doi: 10.1029/JC083iC10p05063.

Reid, J.L. (1979), On the contribution of the Mediterranean Sea outflow to the Norwegian-Greenland Sea, *Deep Sea Res*, *26A*, 1199-1223.

Reid, J. L. (1994), On the total geostrophic circulation of the North Atlantic Ocean: Flow patterns, tracers, and transports, *Prog. Oceanogr*, *33*(1), 1-92.

Teague, W. J., M.J. Carron, and P.J. Hogan (1990), A comparison between the Generalized Digital Environmental Model and Levitus climatologies, *J. Geophys. Res.*, *95*, 7167-7183.

Zenk, W. (1975), On the Mediterranean outflow west of Gibraltar, Meteor Forschungsergeb, 16, 23-24.

**Tables:**

| Experiments | Salinity Trend (psu/decade) | Temperature Trend (C/decade) | Density Trend ($kg/m^3$ /decade) |
|---|---|---|---|
| HYDROBASE2 (Observations) | 0.0298±0.0028 ($r^2$=0.76) | 0.129±0.013 ($r^2$=0.73) | -0.0018±0.0012 ($r^2$= 0.06) |
| REF | 0.0135±0.0015 ($r^2$=0.68) | 0.058±0.008 ($r^2$=0.58) | 0.0002±0.0003 ($r^2$=0.01) |
| WIND | 0.0204±0.0014 ($r^2$=0.85) | 0.089±0.008 ($r^2$=0.80) | -0.0008±0.0003 ($r^2$= 0.13) |
| BUOY+WIND | 0.0312±0.0030 ($r^2$=0.74) | 0.143±0.014 ($r^2$=0.73) | -0.0026± 0.0004 ($r^2$=0.57) |

**Table 1:** Salinity (psu/decade), temperature (ºC/decade) and density ($kg/m^3$/decade) trends at 1100 m between 1955-1993 in the box 1 using the hydrographic profiles of HYDROBASE 2 and the results of REF, WIND, and BUOY+WIND experiments.

| Experiments | Salinity Trend (psu/dec) | Temperature Trend (C/dec) | Density Trend ($kg/m^3$ /dec) |
|---|---|---|---|
| HYDROBASE2 (Observations) | 0.0190±0.0026 ($r^2$=0.53) | 0.097±0.011 ($r^2$=0.64) | -0.0002±0.0008 ($r^2$= 0.00) |
| REF | 0.0094±0.0012 ($r^2$=0.57) | 0.041±0.006 ($r^2$=0.49) | 0.0001±0.0002 ($r^2$=0.01) |
| WIND | 0.0174±0.0011 ($r^2$=0.83) | 0.079±0.006 ($r^2$=0.80) | -0.0010±0.0002 ($r^2$= 0.30) |
| BUOY+WIND | 0.0195±0.0026 ($r^2$=0.55) | 0.092±0.014 ($r^2$=0.56) | -0.0019± 0.0003 ($r^2$=0.53) |

**Table 2:** as Table 1 for 1955-2003.

## Figures:

**Figure 1:** Salinity at 1100 m from GDEM3 climatology on the HYCOM 1/3º Atlantic domain. Gray areas show the 1100 m isobaths. The analysis of the MOW variability is done over the reservoir and its western and northern pathways (Figure 1): the MOW reservoir [8.3ºW, 25ºW, 32ºN, 42ºN] (box 1), the central Atlantic [30ºW, 40ºW, 30ºN, 40ºN] (box 2) for the western pathway, and the Rockall Trough [11.5ºW, 15ºW, 52.5ºN, 57.5ºN] (box 3) for the northern pathway. The white square shows the location of Porcupine Bank.

**Figure 2:** Evolution of salinity, temperature and density in box 1 (Figure 1) at 1100 m for REF (thin black), WIND (gray), and BUOY+WIND (thick black). Vertical dashed lines bound the *Potter and Lozier* [2004] period.

**Figure 3:** Salinity of averaged over $\sigma_2$ = 36.38 kg/m$^3$ and $\sigma_2$ = 36.52 kg/m$^3$ for REF, WIND and BUOY+WIND (left to right) averaged over the period 1955-1970 (a, b, and c) and 1980-1995 (d, e, and f) and the difference of salinity between these two periods (g, h, and i).

**Figure 4:** Transport budget in box 1 (Figure 1) for each experiment: transport at the eastern boundary (dark gray), at the western boundary (thick black), at the northern boundary (light gray), and at the southern boundary (thin black). Transports are positive for a flow going out of the box. Bottom: winter NAO index [*Hurrell*, 1995].

**Figure 5:** Time evolution of the thickness of ten density classes ranging from $\sigma_2$ = 36.04 kg/m$^3$ and $\sigma_2$ = 36.97 kg/m$^3$ averaged over box 2 for a) WIND and c) BUOY+WIND. The evolution of salinity averaged over the same region for the two MOW density classes is given on top. The evolution of the MOW density classes is in light gray while the

evolution of the LSW density classes is in dark gray. Vertical dotted lines bounds the period 1955-1970 and 1980-1995. The number of the layer and their corresponding densities is given on the right panel.

**Figure 6:** Evolution of the LSW density class ($\sigma_2$=36.83 kg/m$^3$) thickness (m) by 5-year bin from 1950 to 2006. White contours are salinity contours of the MOW ($\sigma_2$=36.52 kg/m$^3$). The NAO state is given for each 5-year bin from 1950 to 2004 and for 2005-2006.

**Figure 7:** Evolution of the 3-year running mean a) northward transport, salinity anomaly b) in box 1 and c) in the Rockall Trough (box 3) for BUOY+WIND. To highlight the impact of low and high NAO phases on the MOW circulation, the subtracted mean used for the anomaly is 1955-1995.

**Figure 8:** Evolution of the NAO index (black), the transport index anomaly (red) between the Labrador Sea and the Bermuda Islands lagged by 2 years and the SSH anomaly (reversed) averaged over the box [60-15ºW, 50-65ºN] (green) lagged by 1 year, for a) REF, b) WIND and c) BUOY+WIND.

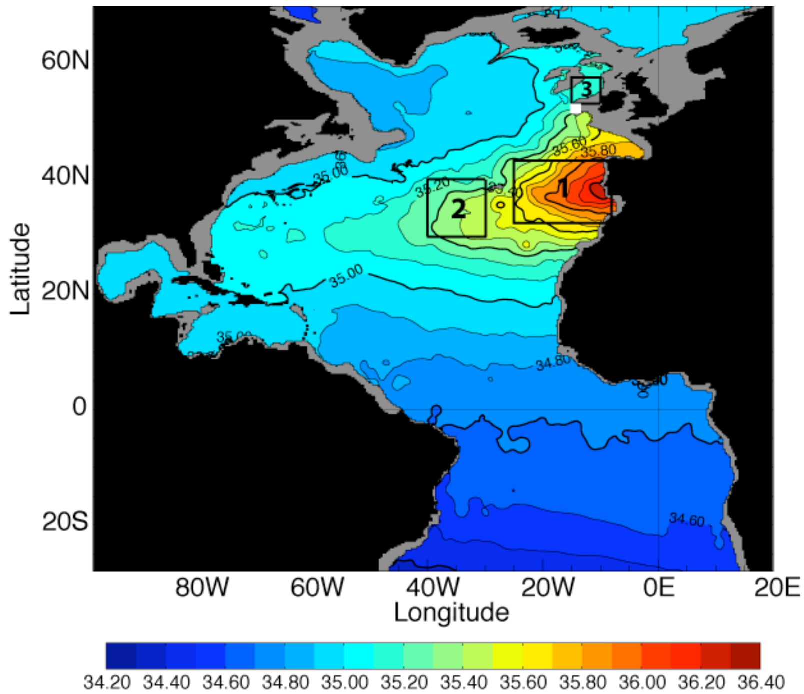


**Figure 1:** Salinity at 1100 m from GDEM3 climatology on the HYCOM 1/3º Atlantic domain. Gray areas show the 1100 m isobaths. The analysis of the MOW variability is done over the reservoir and its western and northern pathways (Figure 1): the MOW reservoir [8.3ºW, 25ºW, 32ºN, 42ºN] (box 1), the central Atlantic [30ºW, 40ºW, 30ºN, 40ºN] (box 2) for the western pathway, and the Rockall Trough [11.5ºW, 15ºW, 52.5ºN, 57.5ºN] (box 3) for the northern pathway. The white square shows the location of Porcupine Bank.

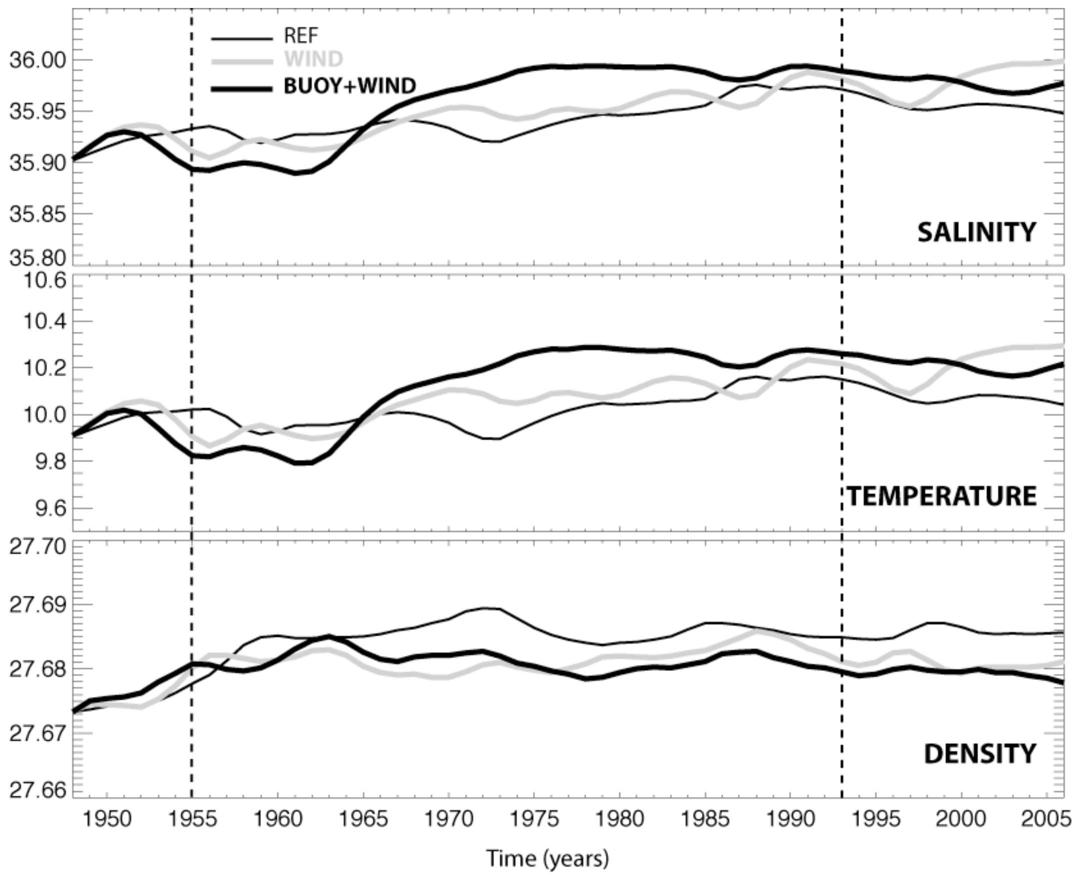


**Figure 2:** Evolution of salinity, temperature and density in box 1 (Figure 1) at 1100 m for REF (thin black), WIND (gray) and BUOY+WIND (thick black). Vertical dashed lines bound the *Potter and Lozier* [2004] period.

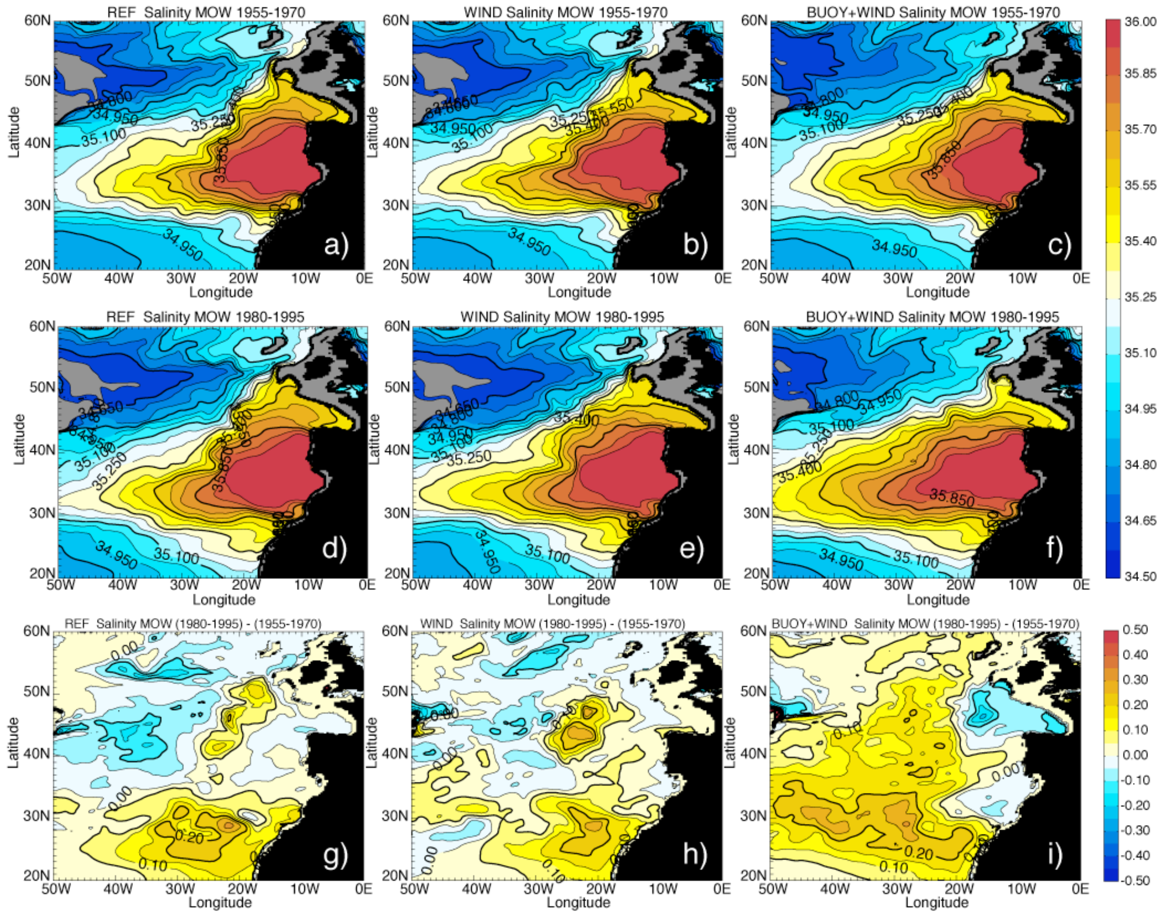


**Figure 3:** Salinity of averaged over $\sigma_2$ = 36.38 kg/m$^3$ and $\sigma_2$ = 36.52 kg/m$^3$ for REF, WIND and BUOY+WIND (left to right) averaged over the period 1955-1970 (a, b and c) and 1980-1995 (d, e and f) and the difference of salinity between these two periods (g, h and i).

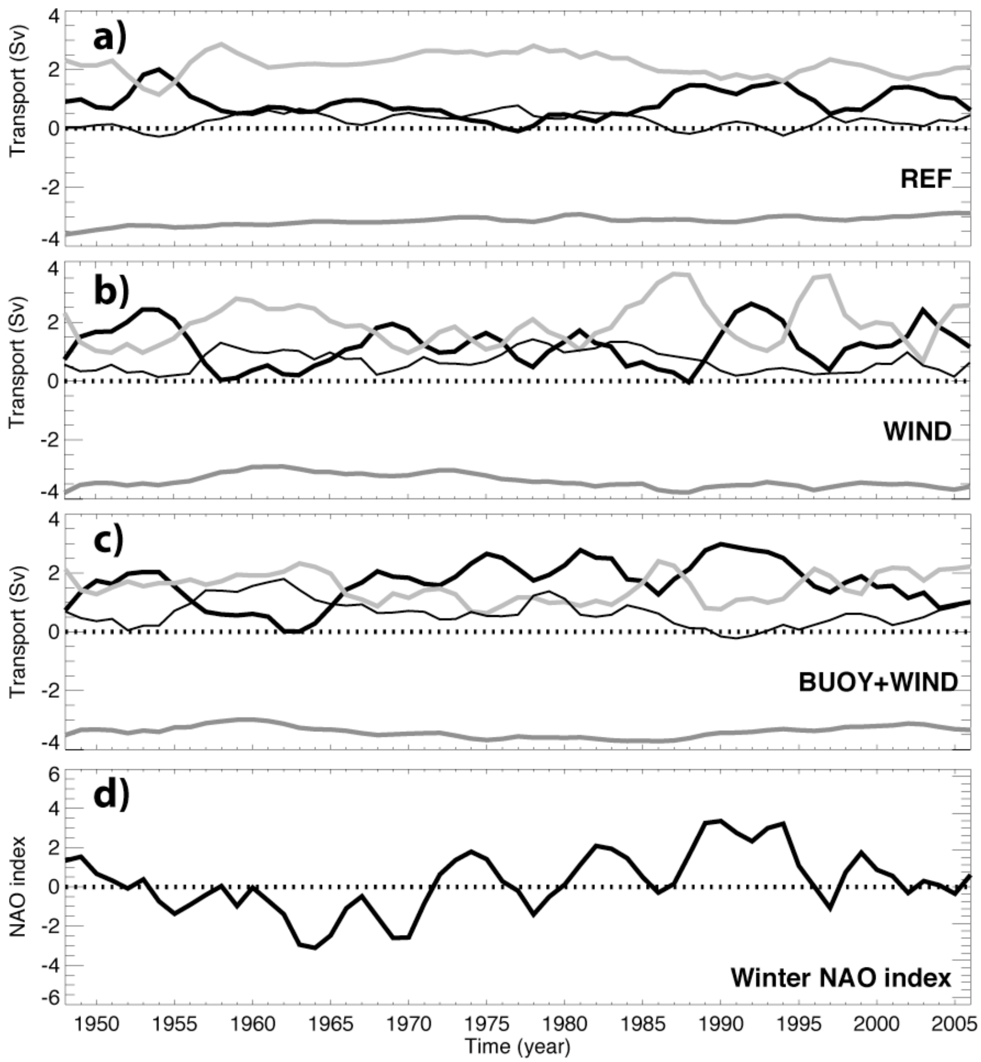


**Figure 4:** Transport budget in the gray box (cf. Figure 2) for each experiment: transport at the eastern boundary (dark gray), at the western boundary (thick black), at the northern boundary (light gray) and at the southern boundary (thin black). Transports are positive for a flow going out of the box. Bottom: winter NAO index [*Hurrell*, 1995].

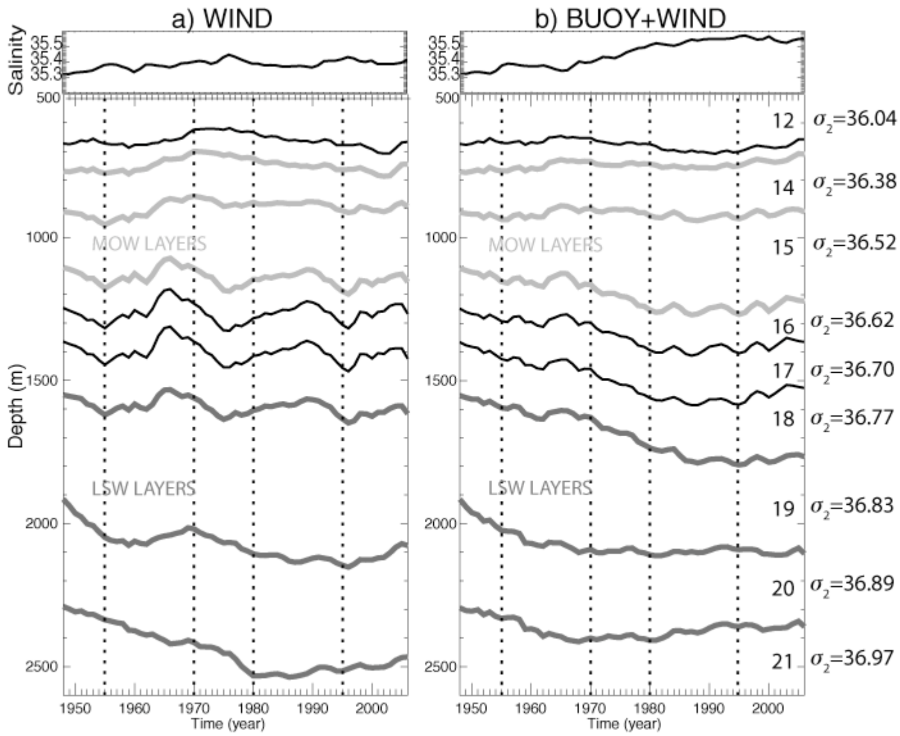


**Figure 5:** Time evolution of the thickness of ten density classes ranging from $\sigma_2$ = 36.04 kg/m$^3$ and $\sigma_2$ = 36.97 kg/m$^3$ averaged over box 2 for a) WIND and c) BUOY+WIND. The evolution of salinity averaged over the same region for the two MOW density classes is given on top. The evolution of the MOW density classes is in light gray while the evolution of the LSW density classes is in dark gray. Vertical dotted lines bounds the period 1955-1970 and 1980-1995. The number of the layer and their corresponding densities is given on the right panel.

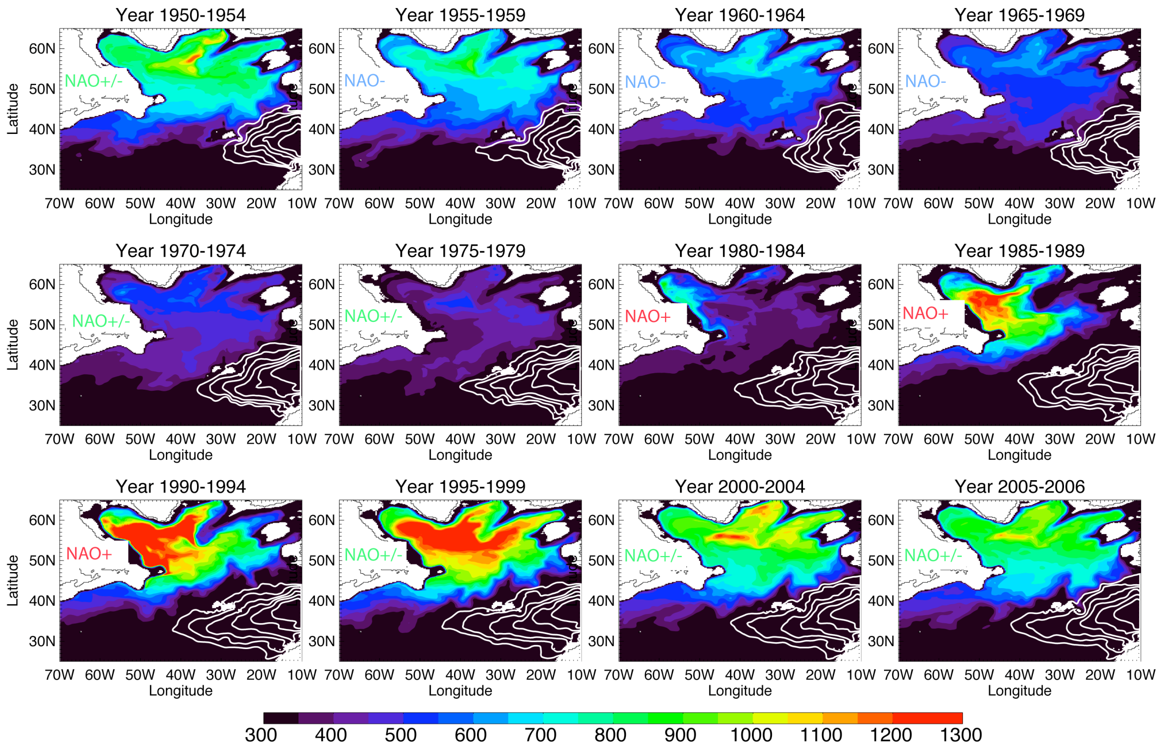


**Figure 6:** Evolution of the LSW density class ($\sigma_2$=36.83 kg/m$^3$) thickness (m) by 5-year bin from 1950 to 2006. White contours are salinity contours of the MOW ($\sigma_2$=36.52 kg/m$^3$) from 35.7psu to 36.2psu. The NAO state is given for each 5-year bin from 1950 to 2004 and for 2005-2006.

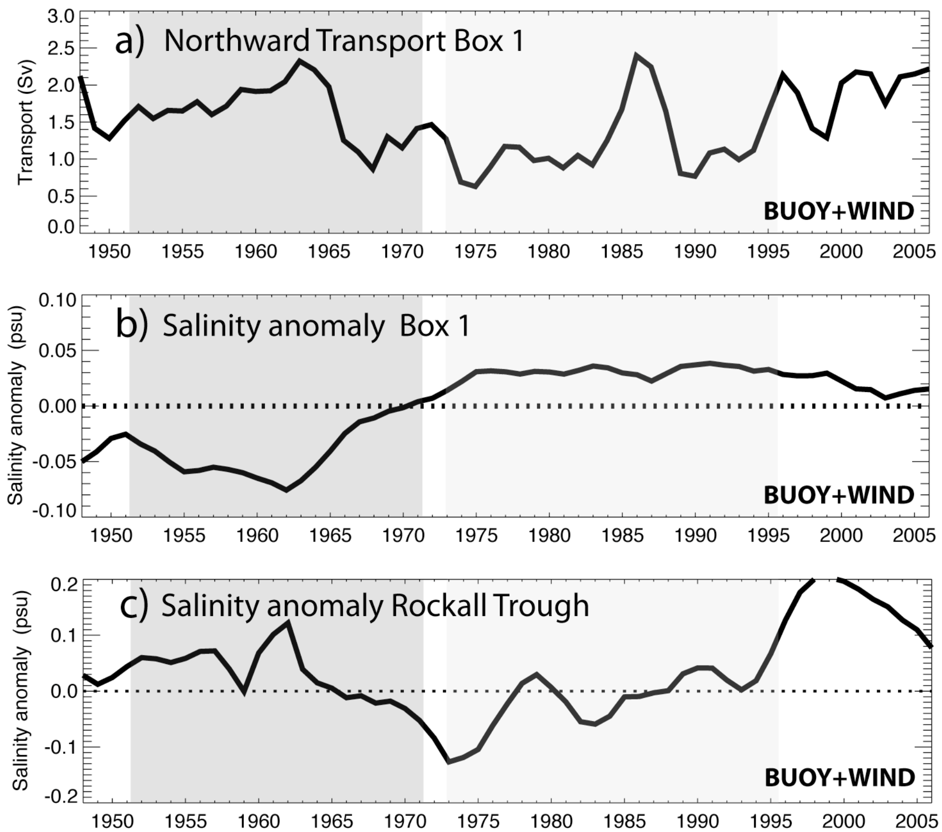


**Figure 7:** Evolution of the 3-year running mean a) northward transport, salinity anomaly b) in box 1 and c) in the Rockall Trough (box 3) for BUOY+WIND. To highlight the impact of low and high NAO phases on the MOW circulation, the subtracted mean used for the anomaly is 1955-1995.

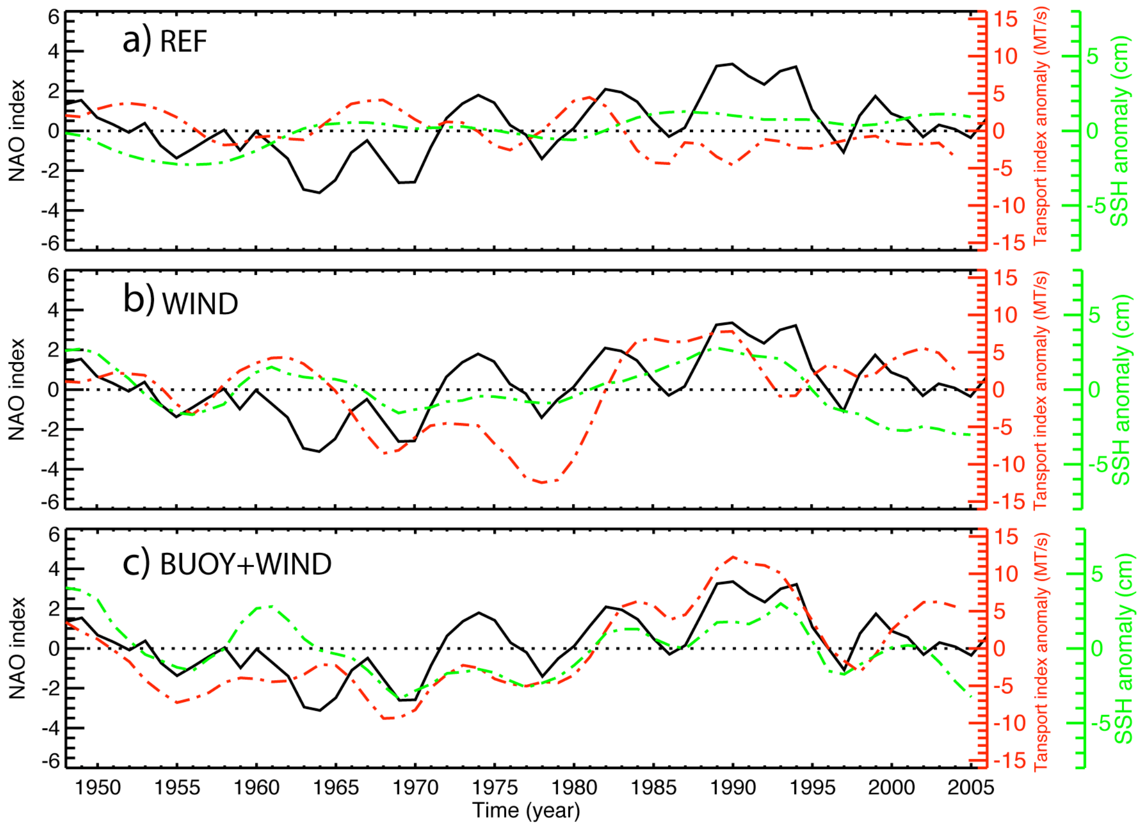


**Figure 8:** Evolution of the NAO index (black), the transport index anomaly (red) between the Labrador Sea and the Bermuda Islands lagged by 2 years and the SSH anomaly (reversed) averaged over the box [60-15ºW, 50-65ºN] (green) lagged by 1 year, for a) REF, b) WIND and c) BUOY+WIND.